Table IX. Atomic Fractional Coordinates with Standard Deviations in Parentheses for 5

atom	x	y	z
W	0.0873 (1)	0.1671 (1)	0.2847 (1)
O1	0.2465 (7)	0.0092 (5)	0.1046 (5)
O2	0.3602 (8)	0.1009 (7)	0.4757 (6)
O3	-0.0227 (9)	0.3413 (5)	0.4683 (7)
C1	-0.0571 (8)	0.0115 (6)	0.3039 (6)
C2	-0.1186 (8)	0.0853 (6)	0.3819 (5)
C3	-0.2679 (8)	0.1365 (6)	0.3196 (7)
C4	-0.1914 (9)	0.2029 (6)	0.2250 (7)
C5	-0.1319 (9)	0.1281 (6)	0.1442 (6)
C6	-0.1737 (9)	0.0175 (6)	0.1928 (6)
C7	-0.3384 (9)	0.0429 (7)	0.2480 (7)
C8	0.170 (1)	0.3006 (6)	0.1728 (7)
C9	0.3106 (9)	0.2724 (6)	0.2529 (8)
C11	0.1879 (8)	0.0679 (6)	0.1690 (6)
C12	0.2634 (8)	0.1247 (6)	0.4073 (6)
C13	0.0160 (9)	0.2805 (6)	0.4011 (6)

data were collected on an Enraf-Nonius CAD4 diffractometer with graphite-monochromated Mo Kα X-radiation. Unit cell parameters were obtained by least-squares fits to the θ values of 75 automatically centered reflections. Data were corrected for Lorentz and polarization effects. Empirical absorption correction was performed for **5** and analytical absorption correction for **3**. $\sigma(F)$ was calculated from $\sigma(F) = [\sigma(I)^2 + (Ik)^2]^{1/2}/2F$, where $k = 0.02$.

The structures were solved by the heavy-atom method. Refinement was by full-matrix least-squares methods, where the function was minimized $\sum w(\Delta F)^2$ with $w = 1/\sigma^2(F)$ and $\Delta F = |F_o| - |F_c|$. The positions of the H atoms were calculated (d(C–H) = 0.95 Å) and included in the refinement with fixed positions and isotropic thermal parameters ($U_H = 0.05$ Å^2). A summary of data collection and processing parameters is given in Table VII. The results of the X-ray analyses are summarized in Tables II–V, VIII, and IX which give selected interatomic distances and angles and the final atomic coordinates. Figures 2 and 3 show the molecular structures.

Acknowledgment. Special thanks go to Rob van de Graaf who participated in this project as a DAAD exchange student.

Registry No. **3**, 12129-25-8; **4**, 117686-87-0; **5**, 117686-88-1; *Z*-cyclooctene, 931-87-3; ethene, 74-85-1.

Supplementary Material Available: Detailed information on the crystal structures of **3** and **5** including figures of the molecular structures and tables of final atomic positional parameters, thermal parameters, and distances and angles (12 pages); listings of observed and calculated structure factors (26 pages). Ordering information is given on any current masthead page.

"Half-Open Metallocenes" of Iron, Ruthenium, and Osmium: Synthesis, Characterization, Photoelectron Spectroscopy, and Theoretical Calculations

Rolf Gleiter,* Isabella Hyla-Kryspin, Manfred L. Ziegler,* and Gertrud Sergeson

Institute für Organische und Anorganische Chemie der Universität, D-6900 Heidelberg 1, West Germany

Jennifer C. Green*

Inorganic Chemistry Laboratory, University of Oxford, Oxford OX1 3QR, Great Britain

Lothar Stahl and Richard D. Ernst*

Department of Chemistry, University of Utah, Salt Lake City, Utah 84112

Received February 9, 1988

The "half-open ruthenocene" and "half-open osmocene" complexes, $M(C_5H_5)(2,4\text{-}C_7H_{11})$ (M = Ru, Os; C_7H_{11} = η^5-dimethylpentadienyl), have been prepared from reductions of $RuCl_3 \cdot nH_2O$ and Na_2OsCl_6, respectively, in the presence of slightly less than 1 equiv of cyclopentadiene and an excess of 2,4-dimethyl-1,3-pentadiene. An X-ray diffraction study of the ruthenium compound has revealed a structure analogous to that found for the isomorphous iron complex, with crystallographically imposed mirror plane symmetry. The structure was refined to agreement indices of $R = 0.030$ and $R_w = 0.028$ in space group D_{2h}^{16}—*Pnma* (No. 62), with $a = 5.917$ (2) Å, $b = 13.124$ (3) Å, $c = 13.501$ (4) Å, and $Z = 4$. The average Ru–C bond distance of 2.178 (3) Å to the cyclopentadienyl ligand was found to be similar to that for the 2,4-dimethylpentadienyl ligand, 2.168 (3) Å. $Ru(C_5H_5)(2,4\text{-}C_7H_{11})$ may readily be protonated by HBF_4, yielding $[HRu(C_5H_5)(2,4\text{-}C_7H_{11})]^+BF_4^-$. Variable-temperature NMR studies demonstrate that the added proton may readily exchange with the four hydrogen atoms attached to the terminal carbon atoms of the pentadienyl ligands. Photoelectron spectroscopy and theoretical calculations have been used to probe the electronic structures of the neutral compounds. On the basis of INDO–MO calculations we have correlated the energy levels and the wave functions of bis(pentadienyl)iron (**1**), (cyclopentadienyl)(pentadienyl)iron (**2**), and ferrocene (**3**). It is predicted that **2** is between **1** and **3** with respect to the energy of the HOMO and the 3d character of the wave functions. The He I and He II photoelectron (PE) spectra of the cyclopentadienyl 2,4-dimethylpentadienyl complexes of iron (**4**), ruthenium (**5**), and osmium (**6**) have been recorded. Assignments for the first bands are based upon INDO calculations on **4**, taking into account the differing Koopmans' defects in the framework of the Green's function technique, as well as relative intensity arguments involving the He I and He II spectra of **4**–**6**. The assignments have been supported through a comparison of the first bands of the PE spectrum of **4** with those of **5** and **6**.

Recently, the physical and theoretical natures of pentadienyl groups, and their metal complexes, have been of interest, especially relative to their better known cyclopentadienyl counterparts.[1] In our own earlier studies,

0276-7333/89/2308-0298$01.50/0

many comparisons between the metallocenes and the "open metallocenes" have been made.[2] Such comparisons are generally complicated by the greatly differing natures of the two classes of complexes. In particular, the "open metallocenes" are sterically very crowded molecules, with substantial interligand nonbonded contacts, which could deleteriously affect the bonding. In addition, they possess much different symmetries relative to the metallocenes, whose high symmetries might prevent some mixing interactions between metal and ligand orbitals from occurring. Finally, the electronic and spin configurations between the two classes of compounds may differ. In an effort to remove such complicating differences, a series of "half-open metallocenes" (for Fe,[3] Cr,[4] Co cation,[5] and ligand adducts of Ti[6] and V[7]) has been prepared, so that the steric, symmetry, and electronic environments have now been equalized. With the syntheses of these half-open metallocenes, the whole series bis(pentadienyl)iron (**1**), (cyclopentadienyl)(pentadienyl)iron (**2**), and ferrocene (**3**) becomes available. This series offers a unique opportunity

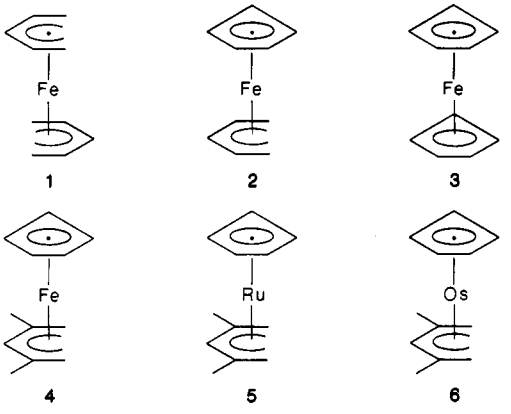

to demonstrate the application of perturbation theory to the study and discussion of the electronic structures of a closely related series of organometallic compounds. Herein we report also the preparations of "half-open" ruthenium and osmium analogues, $M(C_5H_5)(2,4\text{-}C_7H_{11})$ (M = Ru, Os; C_7H_{11} = dimethylpentadienyl), including structural data for the former and comparative photoelectron spectroscopic (PES) studies for the iron, ruthenium, and osmium complexes. The PES studies in particular provide experimental support for the conclusions derived from **1–3** by using perturbation theory.

Experimental Section

All operations involving organometallics were carried out under a nitrogen atmosphere in prepurified Schlenk apparatus or in a glovebox. Nonaqueous solvents were thoroughly dried and deoxygenated in a manner appropriate to each and were distilled immediately before use. Elemental analyses were performed by Desert Analytics Laboratories.

Spectroscopic Studies. Infrared spectra were recorded with a Perkin-Elmer 298 spectrophotometer. Mulls were prepared in a glovebox with dry, degassed Nujol. ^1H and ^{13}C nuclear magnetic resonance spectra were recorded in benzene-d_6 or toluene-d_8 on Varian EM-390, SC-300, and XL-300 spectrometers. Mass spectra (70 eV) were performed on a VG Micromass 7070 double-focusing high-resolution mass spectrometer with the VG Data System 2000. Except for the parent fragment, peaks are only quoted if their relative intensities are at least 10% of the intensity of the strongest peak. He I photoelectron spectra were recorded on a Perkin-Elmer PS18 photoelectron spectrometer with a He Iα lamp as the light source. The recording temperatures ranged from 60 to 80 °C. Calibrations were carried out with Ar and Xe. A resolution of about 20 meV on the argon line was obtained. He II spectra were obtained at the University of Oxford.

(Cyclopentadienyl)(2,4-dimethylpentadienyl)ruthenium, $Ru(C_5H_5)(2,4\text{-}C_7H_{11})$. Into a 100-mL 3-neck flask equipped with nitrogen inlet and magnetic stirring bar is syringed 20 mL of absolute ethanol. The ethanol is then degassed by three freeze–thaw cycles. Ruthenium trichloride hydrate (2.00 g, 7.65 mmol) is dissolved in the ethanol to give a green-brown solution. By microsyringe exactly 0.50 g (7.5 mmol) of freshly distilled cyclopentadiene is added to the stirred ruthenium trichloride solution. This is followed by the addition of 8 mL (70 mmol) of degassed 2,4-dimethyl-1,3-pentadiene and 5.0 g of zinc powder (Fisher), in this order. After the addition of the zinc the reaction mixture becomes quite hot, occasionally leading to reflux. Within 1–2 min the solution turns an ink-blue (Ru^{2+}) but stays that color only for a short time, at which point the solution reverts back to a green-brown. At this point the reaction flask is equipped with a water-cooled condenser and the solution is refluxed under nitrogen for 6 h. On heating, the solution turns black within 1 h. Upon completion of the reflux period the reaction mixture is allowed to cool, and the volatile materials are removed in vacuo leaving a sticky, black residue. The residue is extracted with several 50-mL portions of pentane. The combined extracts are filtered through a Celite disk on a coarse frit to give a light yellow solution. The solution is concentrated to 20 mL, and the flask is placed in a −20 °C freezer. A 70.0% yield of light yellow needle crystals (1.37 g; mp 136–137 °C) is isolated after 3 days.

Anal. Calcd. for $C_{12}H_{16}Ru$: C, 55.15; H, 6.17. Found: C, 55.27; H, 6.32. ^1H NMR (benzene-d_6, ambient): δ 5.31 (s, 1 H); 4.46 (s, 5 H); 2.94 (d, 2 H, J = 2.4 Hz); 1.83 (s, 6 H); 0.19 (d, 2 H, J = 2.4 Hz). ^{13}C NMR (benzene-d_6, ambient): δ 92.5 (d, J = 158 Hz); 92.1 (s); 78.0 (d, J = 176 Hz); 40.5 (t, J = 157 Hz); 27.8 (q, J = 126 Hz). IR (Nujol mull): 3065 (mw); 3044 (m); 3034 (vw); 3026 (vw); 1430 (w); 1414 (vw); 1370 (sh); 1102 (ms); 1033 (m); 1015 (vw); 994 (m); 944 (w); 935 (ms); 865 (m); 806 (s); 773 (vw); 723 (mw).

Mass spectrum (EI): m/e (relative intensity): 69 (12); 114 (12); 139 (10); 141 (12); 164 (19); 165 (21); 166 (26); 167 (43); 169 (27); 229 (19); 230 (22); 231 (27); 232 (44); 234 (25); 243 (11); 244 (14); 245 (24); 247 (14); 253 (10); 254 (11); 256 (33); 257 (46); 258 (59); 259 (100); 260 (69); 261 (63); 262 (66); 264 (23).

(Cyclopentadienyl)(2,4-dimethylpentadienyl)osmium, $Os(C_5H_5)(2,4\text{-}C_7H_{11})$. Degassed, absolute ethanol (15 mL) is syringed into a 100-mL 3-neck flask equipped with magnetic stirring bar and nitrogen inlet. To the ethanol is added by powder funnel 1.00 g (2.18 mmol) of $Na_2OsCl_6 \cdot xH_2O$ (Alfa, 41.57% Os) giving a green-brown solution. This is followed by the addition of 0.135 g (2.05 mmol) of freshly distilled cyclopentadiene, 5.0 mL (42 mmol) of degassed 2,4-dimethyl-1,3-pentadiene and 3.2 g (49 mmol) of zinc powder (Fisher), in this order. After the solution is stirred at room temperature for about 15 min the flask is equipped with a water-cooled reflux condenser and the solution is refluxed under nitrogen for 16 h. On heating the solution turns dark, finally becoming black. Upon completion of the reflux period the remaining volatile materials are removed under vacuum to give a granular brown-black solid. The residue is extracted with six 50-mL portions of pentane resulting in a very light yellow (almost colorless) solution. The combined extracts are filtered through a Celite pad and concentrated to 10 mL in vacuo. After

(1) (a) Böhm, M. C.; Eckert-Maksić, M.; Ernst, R. D.; Wilson, D. R.; Gleiter, R. *J. Am. Chem. Soc.* **1982**, *104*, 2699. (b) Böhm, M. C.; Ernst, R. D.; Gleiter, R.; Wilson, D. R. *Inorg. Chem.* **1983**, *22*, 3815. (c) Ernst, R. D.; Wilson, D. R.; Herber, R. H. *J. Am. Chem. Soc.* **1984**, *106*, 1646.
(2) (a) Ernst, R. D. *Acc. Chem. Res.* **1985**, *18*, 56. (b) Ernst, R. D. *Struct. Bonding (Berlin)* **1984**, *57*, 1.
(3) Elschenbroich, Ch.; Bilger, E.; Ernst, R. D.; Wilson, D. R.; Kralik, M. S. *Organometallics* **1985**, *4*, 2068.
(4) Freeman, J. W.; Wilson, D. R.; Ernst, R. D.; Klendworth, D. P.; Smith, P. R.; McDaniel, M. P. *J. Polym. Sci.*, **1987**, *25A*, 2063.
(5) Ernst, R. D.; Ma, H.; Sergeson, G.; Zahn, T.; Ziegler, M. L. *Organometallics* **1987**, *6*, 848.
(6) Melendez, E. M.; Arif, A. M.; Ernst, R. D.; Ziegler, M. L. *Angew. Chem. Intl. Ed. Engl.* **1988**, *27*, 1099.
(7) (a) Kowaleski, R. M.; Basolo, F.; Trogler, W. C.; Ernst, R. D. *J. Am. Chem. Soc.* **1986**, *108*, 6046. (b) Kowaleski, R. M.; Basolo, F.; Trogler, W. C.; Gedridge, R. W.; Newbound, T. D.; Ernst, R. D. *Ibid.* **1987**, *109*, 4860. (c) Gedridge, R. W.; Hutchinson, J. P.; Ernst, R. D., unpublished results.

5 days at −98 °C, 99 mg (0.28 mmol) of colorless crystals are isolated (13.7% yield; mp 156–157 °C).

Anal. Calcd for $C_{12}H_{16}Os$: C, 41.14; H, 4.60. Found: C, 41.28, H, 4.67. ^1H NMR (benzene-d_6, ambient): δ 5.69 (s, 1 H); 4.62 (s, 5 H); 3.37 (d, 2 H, J = 2.6 Hz); 1.96 (s, 6 H); 0.30 (d, 2 H, J = 2.8 Hz). ^{13}C NMR (benzene-d_6, ambient) δ 90.3 (d, J = 170 Hz); 80.9 (s); 73.4 (d, J = 179 Hz); 29.1 (t, J = 156 Hz); 28.9 (q, J = 127 Hz). IR (Nujol mull): 3096 (vw); 3063 (ms); 1580 (mw); 1451 (vs); 1423 (mw); 1407 (m); 1345 (w); 1279 (m); 1098 (s); 1035 (s); 1012 (vw); 994 (s); 972 (m); 946 (s); 927 (w); 865 (m); 855 (ms); 836 (w); 824 (vs); 664 (sh); 650 (vw); 636 (sh) cm^{-1}. MS (EI, 70 eV): m/e (relative intensity): 174 (11); 266 (10); 268 (12); 280 (11); 282 (10); 290 (12); 291 (15); 292 (24); 293 (19); 294 (19); 295 (14); 296 (12); 318 (33); 320 (63); 322 (91); 332 (12); 333 (21); 335 (26); 346 (65); 349 (97); 350 (100); 351 (58).

Hydrido(cyclopentadienyl)(2,4-dimethylpentadienyl)ruthenium Tetrafluoroborate, $[HRu(C_5H_5)(2,4\text{-}C_7H_{11})]^+BF_4^-$. An amount of 400 mg (1.53 mmol) of $Ru(C_5H_5)(2,4\text{-}C_7H_{11})$ is weighed into a 250-mL 2-neck flask equipped with stirring bar and nitrogen inlet. The yellow solid is then dissolved in 30 mL of diethyl ether, and the ensuing solution is cooled to −78 °C. While the solution is stirred and a vigorous nitrogen flow is maintained, 6.8 mL of a 0.22 M HBF_4 ether solution is added dropwise by syringe. The addition of the tetrafluoroboric acid results in the instant formation of a light yellow, flocculent precipitate. After the solution has warmed to room temperature, the stirrer is removed, allowing a copious amount of light yellow solid to settle in the colorless solution. The ether is removed by syringe, and the solid is washed with small portions of ether and hexanes in this order. Approximately 490 mg of analytically pure $[HRu(C_5H_5)(2,4\text{-}C_7H_{11})]^+BF_4^-$ is isolated in this manner. This corresponds to a 92% yield; however, the reaction appears to be quantitative. Single crystals of this compound can be grown by dissolving the solid in a minimum amount (ca. 5 mL) of dichloromethane and then adding hexanes or ether until the solution just turns cloudy. After ca. 5 days at −20 °C, rod-shaped crystals (mp 204 °C dec) are obtained in this manner. The light yellow title compound is insoluble in most organic solvents. It is, however, very soluble in dichloromethane and nitromethane. Exposure to oxygen and moisture results in decomposition, but the compound may be handled briefly in the atmosphere.

Anal. Calcd for $C_{12}H_{17}BF_4Ru$: C, 41.28; H, 4.91. Found: C, 40.95; H, 4.91. ^1H NMR (dichloromethane-d_2, ambient): δ 6.33 (s, 1 H, H-3); 5.35 (s, 5 H, Cp); 2.27 (s, 6 H, CH_3). ^1H NMR (nitromethane-d_3, 85 °C): δ 6.55 (s, 1 H, H-3); 5.30 (s, 5 H, Cp); 2.31 (s, 6 H, CH_3); −0.74 (br s, 5 H, averaged H-1,5 and Ru-H). ^1H NMR (dichloromethane-d_2, −60.2 °C): δ 6.55 (s, 1 H, H-3); 5.29 (s, 5 H, Cp); 3.07 (d of d, 2 H, H_x-1,5, J = 7.2, 5.0 Hz); 2.20 (s, 6 H, CH_3); −0.28 (d of d, 2 H, H_n-1,5, J = 8.4, 5.0 Hz); −10.08 (quint, 1 H, Ru–H, J = 7.7 Hz). ^{13}C NMR (dichloromethane-d_2, −86 °C): δ 101.2 (s); 98.4 (d, J = 162 Hz); 83.0 (d, Cp, J = 182 Hz); 31.0 (t of d, J = 154, 39 Hz); 27.1 (q, J = 129 Hz). IR (Nujol mull): 3120 (m), 3100 (sh), 3055 (w), 1504 (w), 1414 (w), 1288 (m), 1261 (mw), 1102 (vs), 1067 (vs), 1054 (vs), 1039 (vs), 1005 (s), 972 (mw), 951 (w), 858 (s), 798 (ms), 722 (ms) cm^{-1}.

X-ray Diffraction Study of $Ru(C_5H_5)(2,4\text{-}C_7H_{11})$. Single crystals of this compound were obtained by slowly cooling concentrated solutions in hexane to −20 °C. One well-formed needle-like crystal, of approximate dimensions 0.1 × 0.1 × 0.25 mm, was selected for data collection. Oscillation and Weissenberg photography indicated an orthorhombic unit cell, which was isomorphous with the corresponding iron complex. After the crystal was transferred to a Syntex R3 diffractometer, the unit cell parameters were determined from 25 centered reflections, leading to a = 5.917 (2) Å, b = 13.124 (3) Å, c = 13.501 (4) Å, and V = 1048.40 Å^3 for Z = 4 and λ(Mo K$\bar{\alpha}$) = 0.710 69 Å.

Data were collected in the θ–2θ mode, at a variable scan rate of 2.5–29.5°/min, with $3° \le 2\theta \le 60°$. A total of 1112 reflections were obtained, of which 1060 were considered to be observed ($I > 2.5\sigma(I)$). The intensities of two standard reflections were periodically measured and indicated no change in intensity during data collection. An empirical absorption correction was applied from Ψ scan data by using six reflections in the range $8° \le 2\theta \le 30°$. The relative range in transmission factors was determined to be 0.823–1.000, compared to the calculated linear absorption coefficient of 14.19 cm^{-1}. Systematic absences were consistent with space group D_{2h}^{16}—*Pnma* (No. 62), which was adopted also by the isostructural iron analogue.

Calculations were carried out by using the SHELXTL programs. The ruthenium atom location was obtained from a Patterson map, after which the remaining non-hydrogen atoms were located from a Fourier map. After anisotropic refinement of these atomic parameters (with the molecule possessing crystallographically imposed m symmetry), the hydrogen atoms were located from a difference Fourier map and subjected to isotropic refinement, with a single thermal parameter refined for these atoms. Final refinement led to agreement indices of R = 0.030 and R_w = 0.028. A final difference Fourier map revealed no peaks larger than 0.50 e/Å^3. No unusual intermolecular contacts were observed, and relevant bonding parameters have been tabulated. Anisotropic thermal parameters for the non-hydrogen atoms and least-squares plane information are available as supplementary material. A table of structure factors is also available as supplementary material.

Table I. Comparison of ^1H NMR Data (δ) for $M(C_5H_5)(2,4\text{-}C_7H_{11})$ Complexes

M	H(3)	H(exo)	(CH_3)	H(endo)	C_5H_5
Fe	5.17	2.60	1.77	−0.65	3.88
Ru	5.31	2.94	1.83	0.19	4.46
Os	5.69	3.37	1.96	0.30	4.62
RuH^+	6.55	3.07	2.20	−0.28	5.29

Synthetic and Structural Results and Discussion

Both the "half-open ruthenocene" and the "half-open osmocene", $M(C_5H_5)(2,4\text{-}C_7H_{11})$ (M = Ru, Os), could be prepared by the reduction of appropriate hydrated higher oxidation state chlorides ($RuCl_3$ or Na_2OsCl_6) in the presence of ethanol, a deficiency of cyclopentadiene, and an excess of 2,4-dimethyl-1,3-pentadiene. This particular route was chosen since other studies have suggested that such metal chlorides, when exposed to an excess of cyclopentadiene, will rapidly pick up 1 equiv of ligand, while the second is incorporated at a much slower rate.[8] As cyclopentadiene should be incorporated more rapidly than the more crowded 2,4-dimethylpentadiene, the exposure of a given metal complex to 1 equiv of cyclopentadiene and an excess of 2,4-dimethyl-1,3-pentadiene should result in the incorporation of a single cyclopentadiene-derived ligand (C_5H_5 or C_5H_6) into each metal coordination sphere. On subsequent prolonged heating, each metal complex should then only be able to incorporate a 2,4-dimethyl-1,3-pentadienyl ligand. As both $Ru(C_5H_5)(2,4\text{-}C_7H_{11})$ and $Os(C_5H_5)(2,4\text{-}C_7H_{11})$ were selectively obtained through this procedure[9] (the respective yields being 70 and 14%), this rationale would appear to be correct.[10] Both complexes are air-stable crystalline solids. Pertinent NMR data are compared in Table I.

Although earlier attempts to protonate the "open ferrocenes" seemed to lead to decomposition, one might well expect a heavier congener to possess higher stability. Indeed, the interaction of tetrafluoroboric acid etherate with ether solutions of $Ru(C_5H_5)(2,4\text{-}C_7H_{11})$ at −78 °C

(8) (a) Liles, D. C.; Shaver, A.; Singleton, E.; Wiege, M. B. *J. Organomet. Chem.* **1985**, *288*, C33. (b) Bönnemann, H.; Bogdanovic, B.; Brinkmann, R.; He, D.; Spliethoff, B. *Angew. Chem., Int. Ed. Engl.* **1983**, *22*, 728.

(9) In cases in which too much cyclopentadiene is added some metallocene will also be produced. While their solubilities are similar to those of the half-open metallocenes, they often crystallize first. However, slow and careful crystallization leads to large enough crystals that the small amount of metallocene can generally be removed.

(10) (a) Other related complexes have been reported.[10b–d] (b) Bruce, M. I.; Gardner, R. C. F.; Stone, F. G. A. *J. Chem. Soc., Dalton Trans.* **1979**, 906. (c) Vol'kenau, N. A.; Bolesova, I. N.; Shul'pina, L. S.; Kitaigorodskii, A. N. *J. Organomet. Chem.*, **1984**, *267*, 313. (d) Brammer, L.; Crocker, M.; Dunne, B. J.; Green, M.; Morton, C. E.; Nagle, K. R.; Orpen, A. G. *J. Chem. Soc., Chem. Commun.* **1986**, 1226.

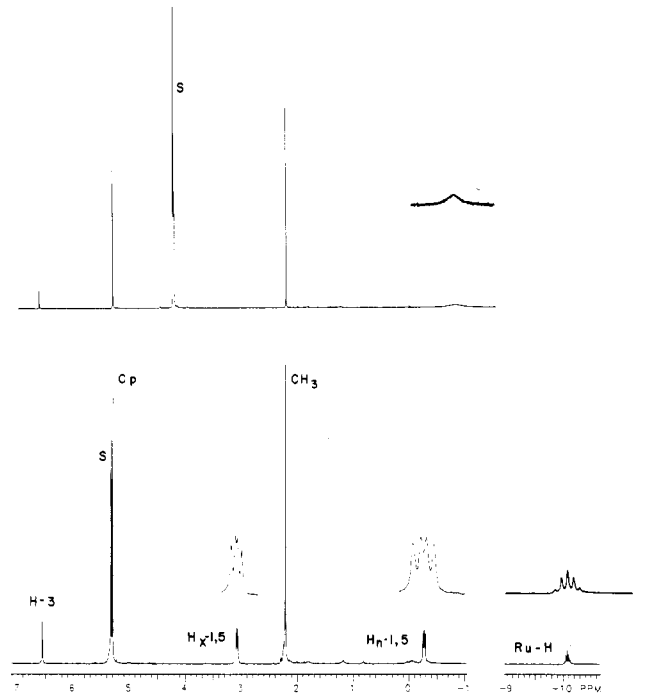

Figure 1. ^{1}H NMR spectra for $[HRu(C_5H_5)(2,4\text{-}C_7H_{11})]^+$ at 85° (top) and −86° (bottom).

affords $[HRu(C_5H_5)(2,4\text{-}C_7H_{11})]^+BF_4^-$ in very high yield (eq 1), and a related complex, $[HRu(C_5Me_5)(\eta^5\text{-}C_8H_{11})]$,

$$Ru(C_5H_5)(2,4\text{-}C_7H_{11}) + HBF_4{\cdot}Et_2O \xrightarrow[-78\ °C]{\text{ether}} [HRu(C_5H_5)(2,4\text{-}C_7H_{11})]^+BF_4^- \quad (1)$$

has also been reported recently (C_8H_{11} = cyclooctadienyl).[11] The reaction is essentially complete within seconds of adding the acid. The light yellow flocculent product is virtually insoluble in ether and readily settles out of solution. It is possible to handle the product in air for short periods of time, but long-term exposure to the atmosphere leads to decomposition. In the room-temperature proton NMR spectrum of $HRu(C_5H_5)(2,4\text{-}C_7H_{11})^+$, only three resonances attributable to the hydrido complex appear. These peaks are assigned to H-3 (6.33 ppm), Cp (5.35 ppm), and CH_3 (2.27 ppm). The absence of spectral lines for the 1,5-position hydrogen atoms and the hydride ligand suggests that an exchange process involving these atoms is occurring. In fact, on cooling to ca. −10 °C, three additional peaks appear at 3.07, −0.28, and −10.08 ppm. These peaks integrate as 2:2:1, and they are easily identified as (to high field) H_x-1,5, H_n-1,5, and Ru–H, respectively. Further cooling results in an increase in signal height of these peaks, and at ca. −40 °C a six-line pattern is frozen out (Figure 1). The highly symmetric peak pattern suggests a molecular structure with mirror plane symmetry, perhaps as in $Ru(C_5H_5)(2,4\text{-}C_7H_{11})$, although it is possible that a formally staggered conformation is adopted. It seems likely that the hydride ligand lies in the mirror plane, as in I. The resonances for H-3, Cp, and

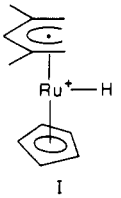

I

Scheme I

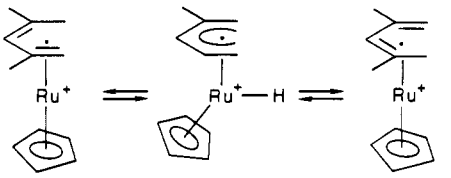

the methyl groups appear as sharp singlets, but both types of 1,5-position hydrogen atoms and the hydride ligand show well-resolved coupling (see Figure 1). The exo protons are seen as a doublet of doublets due to splitting by the endo hydrogen atoms and the hydride ligand with respective coupling constants of 5.0 and 7.2 Hz. A similar doublet of doublets is also observed for the endo protons; the coupling constants here are 5.0 and 8.4 Hz, respectively. These couplings appear to occur by a through-space mechanism, as has been observed in other pentadienyl complexes, and the relatively large coupling constant of ca. 8 Hz indicates that the hydride ligand is in close proximity to these hydrogen atoms. Lack of coupling between the hydride and Cp ligands may indicate that the metal-bound hydrogen is displaced toward the pentadienyl ligand. A structure such as II is consistent with these observations.

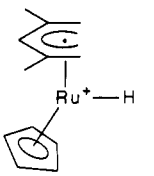

II

The resonance for the metal-bound hydrogen is observed as a quintet at −10.08 ppm. This resonance is split by the four 1,5-position hydrogen atoms with a coupling constant of ca. 7.7 Hz. The four hydrogen atoms on C(1) and C(5) experience coupling not only to the hydride ligand (7.7 Hz) but also to one another. As a result, homonuclear decoupling of the hydride peak results in the collapse of both doublets of doublets (for H(endo) and H(exo)) into simple doublets with a coupling constant of 5.0 Hz. At higher temperatures, one can readily observe scrambling occurring between the hydride ligand and the four hydrogen atoms attached to the terminal carbon atoms. Thus, at 75 °C, a broad resonance integrating for five hydrogen atoms is observed at ca. −0.7 ppm, close to the −0.9 ppm location that represents the weighted average of the five original locations. The ^{13}C NMR data (see Experimental Section) are in accord with these conclusions. Particularly notable is the observation that the CH_2 resonance is observed as a triplet of doublets (J(CH) = 154, 39 Hz). The 39-Hz coupling clearly results from the hydride ligand and once again seems to pinpoint its location as near the open edge of the pentadienyl ligand. Such an orientation (II) is actually quite similar to those found for Lewis base adducts of "half-open metallocenes",[6,7] and for phosphine adducts one observes similar through-space couplings between the phosphorus nuclei and the CH_2 resonances.[6,7,11,12]

The likely exchange pathway is indicated in Scheme I and is consistent with recent observations on related systems. The similar complex $[HRu(C_5Me_5)(\eta^5\text{-}C_8H_{11})]^+BF_4^-$ (C_8H_{11} = cyclooctadienyl)) has been reported[11] but only characterized by room-temperature ^{1}H NMR spec-

(11) Bouachir, F.; Chaudret, B.; Tkatchenko, I. *J. Chem. Soc., Chem. Commun.* **1986**, 94.

(12) Ernst, R. D.; Liu, J.-Z.; Wilson, D. R. *J. Organomet. Chem.* **1983**, *250*, 257.

Table II. Positional Parameters for the Non-Hydrogen Atoms of $Ru(C_5H_5)(2,4\text{-}C_7H_{11})$

atom	x	y	z
Ru	0.13960 (7)	0.75000 (0)	0.50416 (3)
C(1)	-0.0807 (8)	0.8563 (4)	0.5816 (3)
C(2)	0.1267 (7)	0.6532 (3)	0.6332 (2)
C(3)	0.2156 (11)	0.7500 (0)	0.6614 (4)
C(4)	0.2769 (10)	0.5613 (4)	0.6484 (4)
C(5)	0.4414 (14)	0.7500 (0)	0.4117 (6)
C(6)	0.3136 (14)	0.6646 (5)	0.3884 (4)
C(7)	0.1196 (13)	0.6990 (5)	0.3512 (3)

Table III. Positional and Isotropic Thermal Parameters for the Hydrogen Atoms of $Ru(C_5H_5)(2,4\text{-}C_7H_{11})$

atom	x	y	z	U_{iso}, Å^2
H(1A)	-0.1963 (84)	0.8345 (36)	0.6020 (33)	0.073 (6)
H(1B)	-0.0977 (91)	0.9283 (36)	0.5572 (33)	0.073 (6)
H(3)	0.344 (12)	0.7500 (0)	0.6881 (45)	0.073 (6)
H(4A)	0.2451 (90)	0.5145 (36)	0.6004 (35)	0.073 (6)
H(4B)	0.4239 (93)	0.5668 (39)	0.6415 (38)	0.073 (6)
H(4C)	0.2452 (96)	0.5309 (36)	0.7023 (33)	0.073 (6)
H(5)	0.513 (15)	0.7500 (0)	0.4231 (61)	0.073 (6)
H(6)	0.3955 (84)	0.5731 (35)	0.4010 (31)	0.073 (6)
H(7)	-0.0129 (87)	0.8482 (40)	0.3356 (33)	0.073 (6)

troscopy. $[HRu(\eta^5\text{-}C_8H_{11})_2]^+BF_4^-$ has also been reported[11] and characterized by ^1H and ^{13}C NMR spectroscopy (δ -5.62 ppm for the hydride resonance). This compound has been claimed to isomerize reversibly to a (possibly agostic) Ru(dienyl)(diene)$^+$ complex (δ -0.47 ppm). On the basis of our results for $HRu(C_5H_5)(2,4\text{-}C_7H_{11})^+$ (vide supra) and for $HRu(2,4\text{-}C_7H_{11})_2^+$, it seems more likely that their data actually reflect a similar exchange process. However, ground-state "agostic" species have been observed for chromium[13] and isoelectronic manganese[14] complexes, while for $HRe(2,4\text{-}C_7H_{11})(PMe_2(C_6H_5))_3^+$, the ground state is a true hydride complex (δ -10.90 ppm), but presumed coalescence of the hydride ligand with the four hydrogen atoms on the terminal CH_2 groups could not be observed.[14] It is possible that "agostic" intermediates are involved in both interconversions above, but as no direct evidence of their presence could be obtained, they have been omitted from Scheme I.

The facile protonation of $Ru(C_5H_5)(2,4\text{-}C_7H_{11})$ (and $Ru(2,4\text{-}C_7H_{11})_2$) is in great contrast to the relative reluctance of $Fe(C_5H_5)_2$ and $Ru(C_5H_5)_2$ to be protonated. The weakly basic nature of these metallocenes is illustrated by the very low, negative acidity constants of their conjugate acids. For example, the $(H_0)_{1/2}$ values for Cp_2FeH^+ and Cp_2RuH^+ are -7.7 and -5.7, respectively, indicating that both hydrides are clearly very strong acids.[15] The facile transfer of the hydride ligand to the terminal carbon atoms of the pentadienyl ligand(s) leads to useful chemical applications. Thus, exposure to CO, phosphine, or phosphite ligands leads to essentially immediate incorporation of one ligand, concurrent with the formation of an η^4-2,4-dimethyl-1,3-pentadiene ligand.[16] Heating such complexes

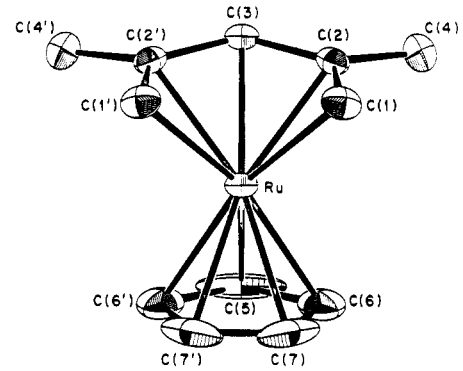

Figure 2. Perspective view and numbering scheme for $Ru(C_5H_5)(2,4\text{-}C_7H_{11})$.

Table IV. Pertinent Bond Distances (Å) and Angles (deg) for $Ru(C_5H_5)(2,4\text{-}C_7H_{11})$

Bond Distances			
Ru-C(1)	2.177 (5)	C(1)-C(2)	1.417 (6)
Ru-C(2)	2.157 (4)	C(2)-C(3)	1.427 (5)
Ru-C(3)	2.170 (5)	C(2)-C(4)	1.512 (7)
Ru-C(5)	2.179 (8)	C(5)-C(6)	1.389 (9)
Ru-C(6)	2.182 (6)	C(6)-C(7)	1.332 (11)
Ru-C(7)	2.175 (5)	C(7)-C(7')	1.339 (14)
Bond Angles			
C(1)-C(2)-C(3)	121.9 (4)	C(5)-C(6)-C(7)	106.3 (6)
C(1)-C(2)-C(4)	120.4 (4)	C(6)-C(5)-C(6')	107.7 (8)
C(2)-C(3)-C(2')	125.9 (5)	C(6)-C(7)-C(7')	109.8 (4)
C(3)-C(2)-C(4)	117.2 (4)		

in the presence of additional two-electron donor ligands leads to the incorporation of two more ligands, during which the diene unit is expelled. Through these routes, both symmetric (L = L') and unsymmetric complexes of formulations $M(C_5H_5)(L)(L')_2^+$ and $M(2,4\text{-}C_7H_{11})(L)(L')_2^+$ may be isolated.

The structure of $Ru(C_5H_5)(2,4\text{-}C_7H_{11})$ was determined by X-ray diffraction and may be seen in Figure 2. Pertinent bonding parameters are contained in Tables II–IV. It would appear that this complex, as well as the iron analogue,[17] exists in the ideally "eclipsed" conformation III as opposed to the "staggered" form IV. Of course, the

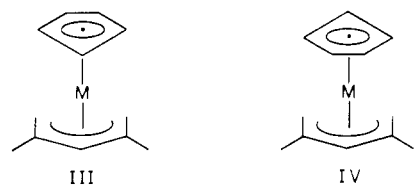

III IV

presence of large cyclopentadienyl thermal parameters may be a result of either substantial thermal motion or the adoption of two slightly staggered conformations. The Ru–C bond distances to the cyclopentadienyl and 2,4-dimethylpentadienyl ligands are similar, averaging 2.178 (3) and 2.168 (3) Å, respectively. The distances observed in $Ru(C_5H_5)_2$,[18] $Ru(2,4\text{-}C_7H_{11})_2$,[2] and $Ru(\eta^5\text{-}C_7H_7)(\eta^5\text{-}C_7H_9)$[19] appear to be slightly longer at 2.196 (3), 2.188 (3), and 2.194 (2) Å, respectively, while the average distance in the eclipsed $Ru(C_5Me_5)_2$[20] is 2.170 (3) Å.

(13) Michael, G.; Kaub, J.; Kreiter, C. G. *Angew. Chem., Int. Ed. Engl.* **1985**, *24*, 502.
(14) Bleeke, J. R.; Kotyk, J. J.; Moore, D. A.; Rauscher, D. J. *J. Am. Chem. Soc.* **1987**, *109*, 417.
(15) (a) Cerichelli, G.; Illuminati, G.; Ortaggi, G.; Giuliani, A. M. *J. Organomet. Chem.* **1977**, *127*, 357. (b) Curphey, T. J.; Santer, J. O.; Rosenblum, M.; Richards, J. H. *J. Am. Chem. Soc.* **1960**, *82*, 5249. (c) Bitterwolf, T. E.; Ling, A. C. *J. Organomet. Chem.* **1972**, *40*, 197.
(16) (a) From $Ru(2,4\text{-}C_7H_{11})_2$, both $Ru(2,4\text{-}C_7H_{11})(\eta^4\text{-}2,4\text{-}C_7H_{12})(CO)^+BF_4^-$ and $Ru(2,4\text{-}C_7H_{11})(CO)_3^+BF_4^-$ have been analytically and spectroscopically characterized, and the monocarbonyl compound through an X-ray structural determination. Various mixed carbonyl/phosphine adducts have also been characterized.[16b] (b) Stahl, L.; Newbound, T. D.; Ernst, R. D., unpublished results.
(17) Kralik, M. S.; Arif, A. M.; Ernst, R. D., unpublished results.
(18) (a) Haaland, A.; Nilsson, J. E. *Acta Chem. Scand.* **1968**, *22*, 2653. (b) Seiler, P.; Dunitz, J. D. *Acta Crystallogr., Sect. B: Struct. Crystallogr. Cryst. Chem.* **1980**, *B36*, 2946.
(19) Schmid, H.; Ziegler, M. L. *Chem. Ber.* **1976**, *109*, 125.
(20) Albers, M. O.; Liles, D. C.; Robinson, D. J.; Shaver, A.; Singleton, E.; Wiege, M. B.; Boeyens, J. C. A.; Levendis, D. C. *Organometallics* **1986**, *5*, 2321.

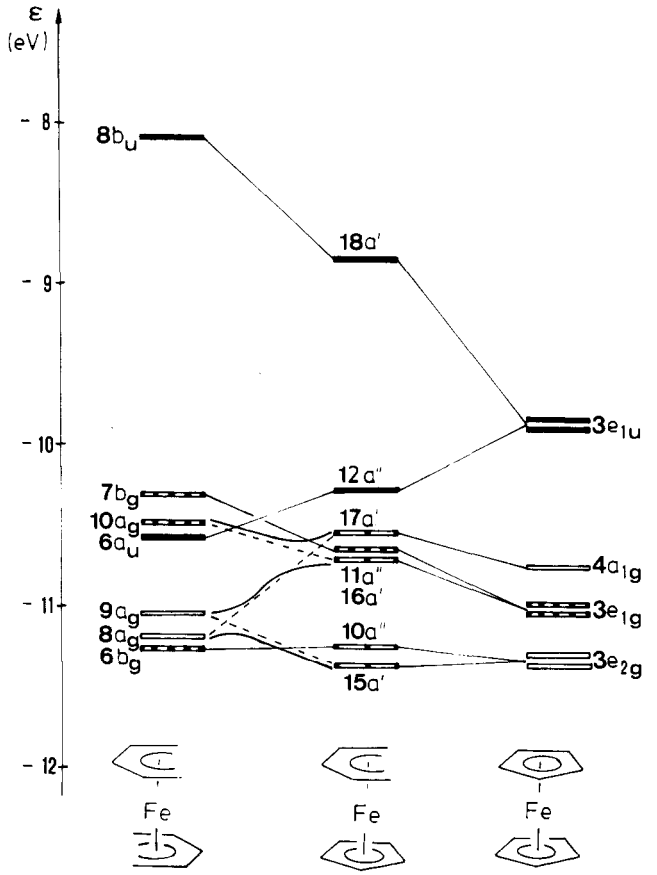

Figure 3. Correlation diagram between the highest occupied MO's of **1** (left), **2** (center), and **3**. Full bars indicate MO's localized on ligands; empty bars indicate MO's localized on metal.

Both ligands, defined by their metal-bound carbon atoms, are relatively planar, to within 0.006 Å for the cyclic ligand, and 0.033 Å for the acyclic ligand. The methyl groups bend down toward the ruthenium atom by 11.6° (0.30 Å), which is similar to values observed in other complexes.[2b] An angle of 7.5° exists between the two ligand planes, such that the terminal pentadienyl carbon atoms are closest to the C_5H_5 plane, while the central pentadienyl carbon atom is furthest. While the average pentadienyl C–C distance of 1.422 (4) Å seems longer than that for the cyclopentadienyl ligand (1.356 (5) Å), this may simply be a result of the high librational motion of the cyclopentadienyl ligand. In fact, electron diffraction results for ruthenocene[18] indicate a C–C bond distance of 1.439 (2) Å. While carbon–carbon bond distances in pentadienyl ligands generally fall in two (delocalized) sets, the "external" one being shorter than the "internal" one, a definitive distinction cannot be made in the present case. As in the case of other pentadienyl complexes, attachment of a methyl group to the central atom of a given C–C–C linkage results in a contraction of that angle, cf. C(1)–C(2)–C(3) = 121.9 (4)° vs C(2)–C(3)–C(2′) = 125.9 (5)°. A C–CH_3 bond distance of 1.512 (7) Å was observed.

Ground-State Properties of 2. To understand the electronic structures of **4**, **5**, and **6** in their ground and various ionic states, we shall first consider the electronic structure of the parent compound **2** and correlate its highest occupied MO's with those of **1** and **3**.

In Figure 3 we have drawn a correlation diagram between the highest occupied MO's of **1–3**. The orbital sequence corresponds to that obtained from INDO-type calculations[21] on **1–3** for which geometrical parameters from structural studies on **1**, **3**, and **4** (or close relatives) have been employed.[22] The wave functions that correspond to the seven highest occupied MO's of **1–3** are compared in Figure 4. To understand the correlations given in Figures 3 and 4 we have to focus on three main points: (i) the in-phase and out-of-phase relationships of the 2pπ MO's on the terminal carbon atoms of the pentadienyl units in **1** (these relationships will determine, according to the rules of perturbation theory,[23] whether a MO which is mainly localized on the ligands will be stabilized or destabilized when the distance between centers **1** and **5** is reduced); (ii) the change in the metal character of a MO, and (iii) the bonding–antibonding relationships between metal and ligand when going from **1** to **3**. The MO's of **1** with strong ligand character are $8b_u$ and $6a_u$, and to a lesser extent $10a_g$ and $7b_g$.[1a,24] Allowing the terminal carbon centers to approach each other in such a way that only one ring is closed first, we expect from the phase relationship a stabilization of $8b_u$ and $10a_g$ and a destabilization of $7b_g$ and $6a_u$. This expectation is met with the exception of $7b_g$. The expected destabilization of $7b_g$ is overcompensated for by a stronger in-phase interaction between the ligand and metal functions in **2** compared with **1**. For the transformation of **2** to **3** the same pattern holds for the four MO's just discussed. As a net result we obtain a strong stabilization of the HOMO due to the ring closure and a slighter stabilization of $10a_g$ and $7b_g$ due to a stronger metal–ligand interaction. Finally, a considerable increase of the metal character is observed in the series $6b_g$–$10a''$–$3e_{2g}$, even though little change in energy occurs.

The take-home lesson of the correlation between **1** and **3** is that **2** is indeed intermediate between **1** and **3**. With respect to energy and the wave function of the HOMO (18a′), it resembles **1**. It shows, however, three MO's (17a′, 15a′, 10a″) with very high 3d character. In this respect it is closer to **3**. This latter result is especially important for a consideration of the cationic states of **2** because wave functions that are highly localized at the metal center will experience large Koopmans' defects on the order of 3–4 eV. Thus for **2** we expect in the low energy region of the PE spectrum four peaks due to the ionizations for 18a′, 17a′, 15a′ and 10a″, while in **1** and **3** only three peaks are found at low ionization energies. The three peaks of **1** include an ionization from one high-lying ligand orbital ($8b_u$) and two strongly localized metal orbitals ($8a_g$, $9a_g$) which are characterized by large Koopmans' defects, while for **3**, all three peaks can be attributed to strongly localized metal orbitals ($3e_{2g}$, $4a_{1g}$)[25] which again experience large Koopmans' defects. The absence of a similar high-lying ligand orbital in **3** arises from the formation of an extra carbon–carbon bond in the cyclopentadienyl ligands relative to the pentadienyl ligands, which brings about substantial stabilization of the $3e_{1u}$ orbital in **3** relative to $8b_u$ in **1** and 18a′ in **2**.

PE Spectra of 4–6. The He I and He II PE spectra of **4–6** are shown in Figure 5, and the data are summarized

(21) Böhm, M. C.; Gleiter, R. *Theor. Chim. Acta* **1981**, *59*, 127, 153.

(22) (a) Wilson, D. R.; Ernst, R. D.; Cymbaluk, T. H. *Organometallics* **1983**, *2*, 1220. (b) Bohn, R. K.; Haaland, A. *J. Organomet. Chem.* **1966**, *5*, 470. (c) Ernst, R. D.; Wilson, D. R.; Kralik, M. S.; Arif, A. M., unpublished results.

(23) Heilbronner, E.; Bock, H. *Das HMO Modell und seine Anwendung*; Verlag Chemie: Weinheim, 1968. Dewar, M. J. S.; Dougherty, R. C. *The PMO Theory of Organic Chemistry*; Plenum: New York, 1975.

(24) Gleiter, R.; Böhm, M. C.; Ernst, R. D. *J. Electron Spectrosc. Relat. Phenom.* **1984**, *33*, 269.

(25) Evans, S.; Green, M. L. H.; Jewitt, B.; Orchard, A. F.; Pygall, C. F. *J. Chem. Soc., Faraday Trans. 2* **1972**, *68*, 1874. Rabalais, J. W.; Werme, L. O.; Bergmark, T.; Karlsson, L.; Husain, M.; Siegbahn, K. *J. Chem. Phys.* **1972**, *57*, 1185. Cauletti, C.; Green, J. C.; Kelly, R.; Powell, P.; van Tilborg, J.; Robbins, J.; Smart, J. *J. Electron Spectrosc. Relat. Phenom.* **1980**, *19*, 327.

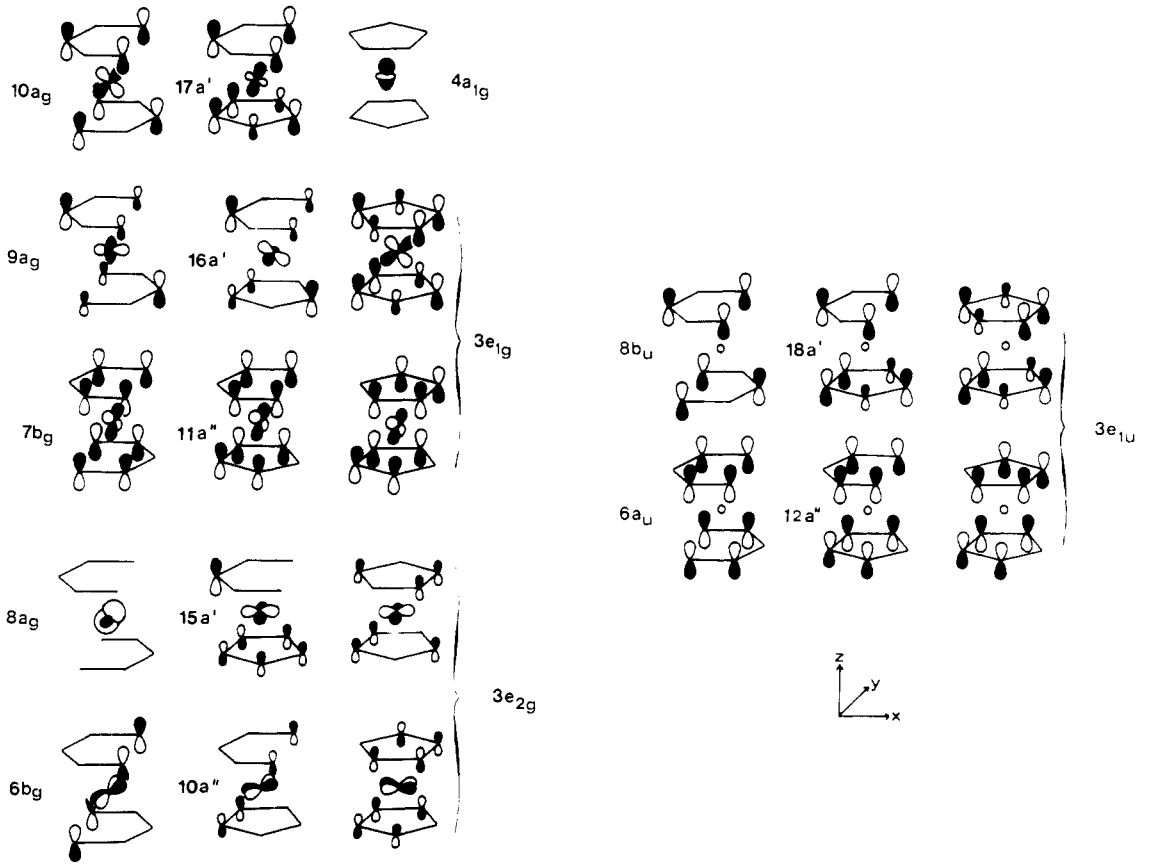

Figure 4. Correlation between the wave functions of **1**, **2**, and **3**. The MO's are drawn schematically, and the avoided crossing between $9a_g$ and $8a_g$ is indicated.

Table V. Ionization Energies ($I_{v,j}$) and Assignments of the First He I Bands of 4-6

compd	band	$I_{v,j}$ (eV)	assignt[a]
4	1	6.65	15a′
	2	6.9	10a″
	3	7.3	17a′
	4	8.3	18a′
	5	9.0	12a″
	6	9.3	16a′
	7	9.5	11a″
	8	10.4	14a′
5	1	7.05	15a′
	2	7.3	10a″
	3	7.9	17a′
	4	8.3	18a′
	5	8.6	12a″
	6	9.6	16a′
	7	9.9	11a″
	8	10.65	14a′
6	1	6.9	15a′
	2	7.30	10a″
	3	8.1	17a′
	4	8.6	18a′
	5	8.8	12a″
	6	9.8	16a′
	7	10.1	11a″
	8	10.7	14a′

[a] The numbering scheme of the irreducible representations refers to the valence orbitals of **2** (cf. Figures 3 and 4).

in Table V. The spectrum of **4** differs from those of **5** and **6** primarily with regard to the shape of the bands. The PE spectra of **5** and **6** show a shoulder and a sharp peak around 7 eV, followed by broad bands between 8 and 9 eV. The PE spectrum of **4** shows three peaks (bands 1–3) centered at 7 eV, followed by two peaks around 9 eV.

To assign the PE spectra of **4**–**6** we proceed both empirically and through the use of MO calculations. Empirically one can compare the band intensities of the He I PE spectra with those of the He II PE spectra, making use of the observation that the PE cross sections of metal d orbitals and ligand MO's differ significantly.[26] Bands associated with ionizations from MO's of metal d character are considerably enhanced in the He II spectra relative to those bands which originate from ligand orbitals. In fact, a comparison of the He I and He II intensities for **4** reveals a strong enhancement of the peak at 6.9 eV (bands 1–3) with respect to the peak at 8.3 eV (band 4). A slight enhancement is also encountered for bands 6 and 7. The comparison of the He I and He II spectra for **5** and **6** also reveals a strong increase in intensity for bands 1 and 2 and to a lesser degree for band 3. As in the case of **4**, the

Table VI. Orbital Energies, ϵ_i, Ionization Energies, I_j^{GF}, MO Type, and Iron 3d Contribution to the MO's of 4 According to an INDO Calculation

MO	i[a]	ϵ_i (eV)	I_j^{GF} (eV)	% Fe	MO type
36	18a′	−8.79	8.01	13	π(Cp), π(pent)
35	12a″	−9.88	9.32	4	π(Cp), π(pent)
34	17a′	−10.34	7.92	50	$3d_{z^2}$, $3d_{x^2-y^2}$, $3d_{xz}$, π(Cp), π(pent)
33	11a″	−10.54	9.77	30	π(Cp), π(pent), $3d_{xz}$, $3d_{xy}$
32	16a′	−10.59	9.53	36	π(Cp), π(pent), $3d_{xz}$, $3d_{x^2-y^2}$, $3d_{z^2}$
31	10a″	−11.12	7.98	78	$3d_{xy}$, $3d_{xz}$, π(pent), π(Cp)
30	15a′	−11.23	7.89	70	$3d_{x^2-y^2}$, $3d_{xz}$, $3d_{z^2}$, π(Cp), π(pent)
29	14a′	−11.43	8.98	45	π(Cp), π(pent), $3d_{z^2}$, $3d_{x^2-y^2}$, $3d_{xz}$

[a] The numbering scheme of the irreducible representations corresponds to the valence electrons of **2**.

(26) Connor, J. A.; Derrick, L. M. R.; Hall, M. B.; Hillier, I. H.; Geret, M. F.; Lloyd, D. R. *Mol. Phys.* **1974**, *28*, 1193.

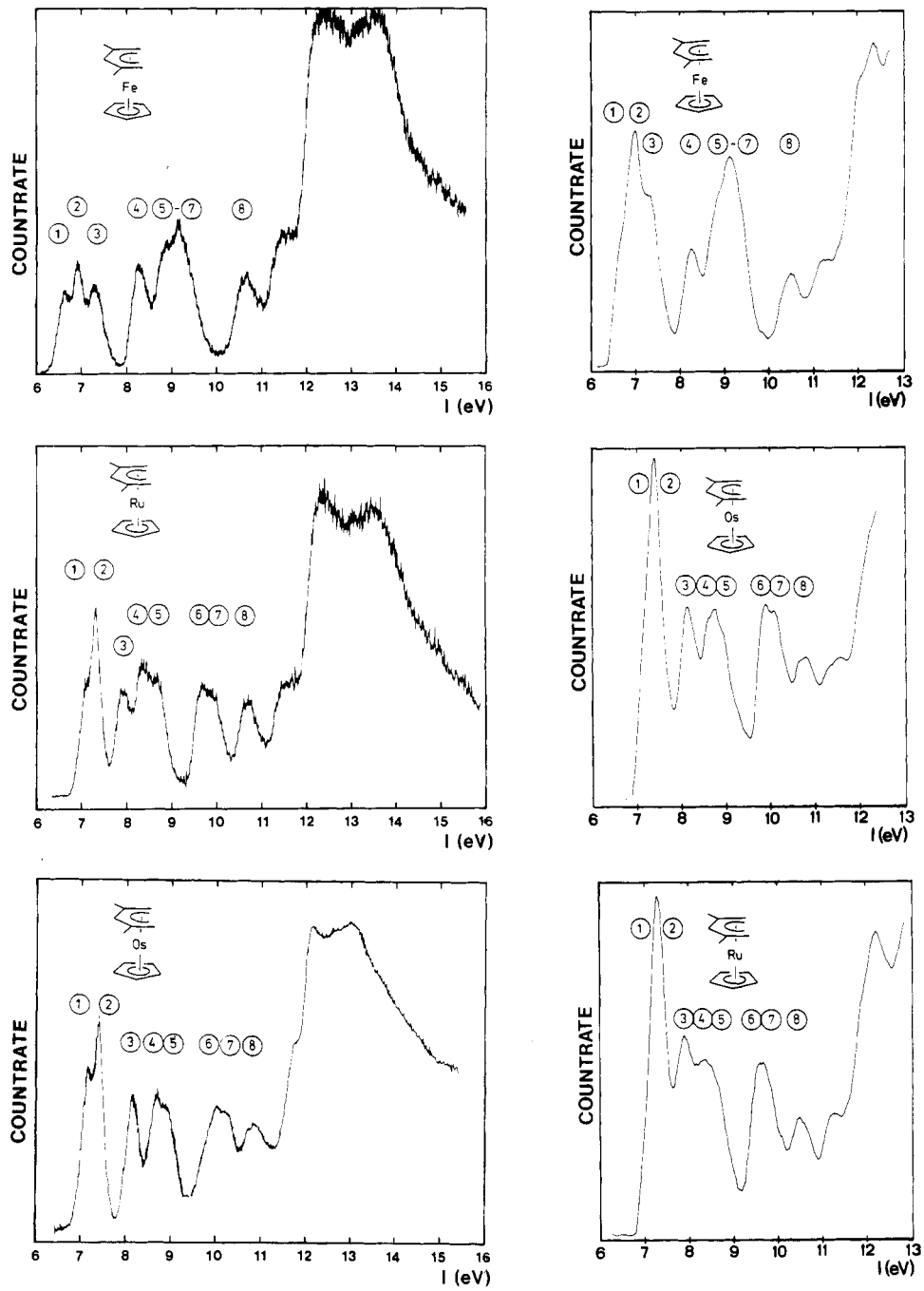

Figure 5. He I (left) and He II (right) PE spectra of **4**–**6**.

intensity ratios of the higher bands vary only slightly. However, an increase in intensity of bands 6 and 7 is noticeable relative to bands 4, 5, and 8. These changes have led us to assign bands 1–3 and bands 6 and 7 to ionizations from MO's with substantial d character, while bands 4 and 5 are ascribed to ionizations from ligand MO's. This comparison also suggests that the highest metal character should reside in bands 1 and 2 followed by 3, 6, and 7.

Our calculations are based on the INDO formalism[21] using the Greens function technique. For the geometrical parameters we used those determined by an X-ray study of **4**.[2a] The iron–carbon distances for each of the ligands were assumed to be 2.06 Å. Using the same approximations for the solution of the inverse Dyson equation[27] as applied in previous studies,[24] we obtain the results listed in Table VI and Figure 6. For the sake of simplicity we adopt the same numbers for the orbitals as in the case of **2**. The calculations on **4** predict large Koopmans' defects for the orbitals 15a′, 10a″, and 17a′, which are mainly localized at the metal (see Table VI, Figure 4, and Figure 6). The states arising from 15a′, 10a″, and 17a′ are predicted to occupy the first peak (bands 1–3) around 7 eV. For 16a′ and 11a″ the metal character is predicted to be 30% while the two highest occupied MO's (18a′ and 12a″) are strongly localized at the ligands. For the two ligand MO's, as well as for 16a′ and 11a″, the predicted Koopmans' defects (Figure 6) are on the order of 0.5–1 eV, while 14a′ shows a relatively large Koopmans' defect due to its large metal contribution (45%).

Contrasting the arguments derived from the comparison of the intensities of the He I and He II spectra and our calculations yields good agreement insofar as the three close-lying ionic states around 7 eV are due to ionizations from MO's with strong metal character. Our comparison between the intensities of the He I and He II spectral

(27) Dyson, F. J. *Phys. Rev.* **1949**, *75*, 486.

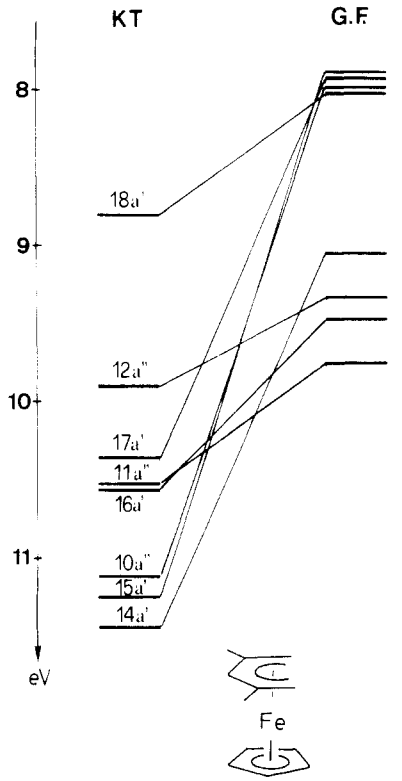

Figure 6. Calculated ionization energies for **4** assuming the validity of Koopmans' theorem (KT) and using the inverse Dyson equation (G.F.), according to an INDO calculation.

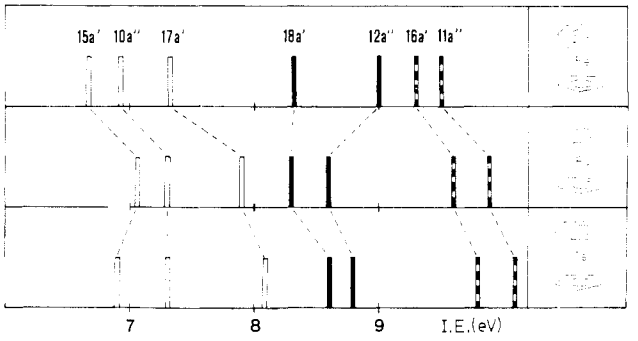

Figure 7. Correlation between the first bands in the PE spectra of **4–6**. Full bars indicate bands that originate from ligand MO's; empty bars correspond to bands that originate from metal MO's.

bands suggests an assignment of 15a′ and 10a″ to the first two bands and 17a′, with smaller metal character, to band 3. For the next two ionic states we assign the ligand orbitals 18a′ and 12a″ followed by 16a′, 11a″, and 14a′. This assignment is based on the comparison of the He I–He II intensities but is partly at variance with the calculations.

The main discrepancy between the empirical assignment and the calculations is the position of the ionic state ascribed to 14a′. Additionally, the 18a′ state is predicted to be too close to 15a′, 10a″, and 17a′. The present assignment of 14a′ to an energy between 10 and 11 eV is consistent with the results on **1** and its congeners.[1a,28] Since the wave function of 14a′ can be described as a linear combination between the lowest π-orbitals of both ligands and 3d functions (see Table VI), it seems reasonable that this level should have a rather high ionization energy.

In Figure 7 a correlation for the first bands of the PE spectra of **4–6** is presented. On the basis of precedent involving PE spectra for various metallocenes,[2,28] a shift to higher ionization energies was expected for those MO's with strong metal character or with a strongly bonding interaction between metal and ligand. This expectation is verified for bands 15a′, 10a″, 17a′, 16a′, and 11a″ given the assignments in Table V and Figure 7. The effects are large in passing from **4** (Fe) to **5** (Ru) but smaller from **5** (Ru) to **6** (Os), in line with earlier observations.[25,28] The only uncertainty remaining relates to the sequence of the first two bands. Due to the strong overlap in all three compounds, further experiments (e.g., ESR investigations on the radical cations) will be required to determine the proposed sequence.

Acknowledgment. R.D.E. expresses his gratitude for support of this research from the National Science Foundation. R.G. wishes to thank the Deutsche Forschungsgemeinschaft for their support. R.D.E. and R.G. are further grateful to NATO for a travel grant, which made this work possible. I.H.-K. is grateful to the Stiftung Volkswagenwerk for financial support.

Registry No. 1, 74910-62-6; **2**, 96645-47-5; **3**, 102-54-5; **4**, 98705-31-8; **5**, 117687-81-7; **6**, 117687-82-8; $[HRu(C_5H_5)(2,4\text{-}C_7H_{11})]^+BF_4^-$, 117709-57-6; $RuCl_3$, 10049-08-8; Na_2OsCl_6, 1307-81-9; cyclopentadiene, 542-92-7; 2,4-dimethyl-1,3-pentadiene, 1000-86-8.

Supplementary Material Available: Tables of anisotropic thermal parameters and least-squares planes (2 pages); a listing of structure factors (7 pages). Ordering information is given on any current masthead page.

(28) Stahl, L.; Ma, H.; Ernst, R. D.; Hyla-Krypsin, I.; Gleiter, R., Ziegler, M. L. *J. Organomet. Chem.* **1987**, *326*, 257. Böhm, M. C.; Gleiter, R. *Angew. Chem.* **1983**, *96*, 334; *Angew. Chem., Int. Ed. Engl.* **1983**, *22*, 329.